Single-channel dose-response studies in single, cell-attached patches

Anthony Auerbach
State University of New York at Buffalo, Department of Biophysical Sciences, Buffalo, New York 14214 USA

ABSTRACT A method for carrying out dose-response studies of ion channel currents in cell-attached patches has been devised. Patch pipettes are filled at the tip with a solution containing one concentration of ligand and then backfilled with another. The concentration of ligand at the membrane is described as a function of time by the equation for diffusion in a cone, allowing response vs. time data to be transformed into a dose-response curve. For *Xenopus* myocyte cholinergic receptors, examples of the use of this method are given for several concentration-dependent reactions including blockade by the local anesthetic QX-222, activation by acetylcholine, and modulation of current amplitude by sodium ions. Several methods of analyzing the nonstationary channel kinetics are presented, including a pseudo-stationary approach that uses interval likelihood maximization.

INTRODUCTION

Dose-response studies have contributed valuable information about ion channel gating and permeation mechanisms. In single-channel patch clamp experiments, changing the concentration of agonists, antagonists, or ions is most readily accomplished with excised patches where a single patch can be superfused with multiple solutions. However, it may be desirable to carry out the dose-response study with the membrane in the cell-attached configuration where cell metabolism and, presumably, membrane structure are preserved. For example, some preparations resist the formation of outside-out patches, and it has been shown that channels in outside-out patches can exhibit functional properties that differ from those in cell-attached membranes (Covarrubias and Steinbach, 1990).

Because channel properties can vary on a patch-to-patch basis, it is preferable to carry out dose-response analyses on a single patch. Several groups have published methods of exchanging pipette solutions while in cell-attached or whole-cell mode (Cull-Candy et al., 1980; Neher and Eckert, 1988; Tang et al., 1990), but these have required that the new solution exchange fully and reach steady state before the channel currents can be quantified. Here I describe a very simple method for changing the concentrations of ligands in a cell-attached patch. As in the nystatin-permeabilized patch paradigm (Horn and Marty, 1988), pipettes are filled at the tip with one solution and then backfilled with another. The concentration of ligand at the pipette tip as a function of time can be quantified, as can the kinetic and conductance properties of channels exposed to changing concentrations of these ligands. A brief report of this method has appeared in abstract form (Auerbach, 1991*a*).

METHODS

Pipettes

Pipettes were pulled from borosilicate blanks on a Sachs-Flaming P2 puller. The temperature of the block that holds the filament was monitored to insure a consistent pipette shape. Pipette tips were firepolished on a home-made forge (no air puff) so that the final orifice diameter was 0.5–1.0 μm (Ruknudin et al., 1991). Pipette shape was measured from digitized video images (optical magnification = 200×). The deviation from a conical shape was quantified by determining the divergence angle (ϕ) for segments of pipette as a function of distance from the orifice (x):

$$\phi = 2 \cdot \tan^{-1}[(r_2 - r_1)/(x_2 - x_1)],$$

where r_2 and r_1 are pipette radii (outer dimension) measured at axial distances x_2 and x_1.

The tips were filled by capillary action. Filling was monitored by videomicroscopy at a total magnification of 40×. The fill height, defined as the distance from the pipette orifice to the meniscus, ranged from 1.3–2.1 mm and was measured to an accuracy of 25 μm. Shanks were backfilled by syringe. A small bubble was trapped between the tip and shank solutions that was quickly dislodged by flocking the pipette. A stopwatch was started at the moment the two solutions joined, marking the start time of the experiment. Pipettes in which no bubble formed were discarded.

Fluorescence measurements

Pipette tips were filled with normal saline, and were backfilled with 50 μM carboxyfluorescein in normal saline. Video images (Dage-MTI SIT camera) of the tip region fluorescence were recorded on a standard VCR at 1 min intervals; to minimize bleaching, the objective was rotated away between measurements. For each time point, a single frame was digitized (within 0.5 s of repositioning the objective) and the mean intensity of a 15 × 15 μm region within the lumen of the pipette was determined. For the calibration curve, pipettes were filled throughout with carboxyfluorescein. For both diffusion and calibration experiments, the diameter of the pipette in the measured region (i.e., the pathlength) was 15 μm (~150 μm from the pipette orifice).

0006-3495/91/09/660/11 $2.00

Electrophysiology

The experimental preparation was myocytes from stage 20–22 *Xenopus* somites. Cells were maintained in tissue culture (60% Leibowitz plus 0.5% serum) for 24 h at 24 °C. Only data from the lower conductance class (γ40; Auerbach and Lingle, 1987) of cholinergic channel are presented here. Unless otherwise noted, the experimental temperature was 18°C, and the pipette potential was +40 mV (estimated V_m = −115 mV). The standard physiological saline was (in mM): 110 NaCl, 2 KCl, 1 $CaCl_2$, 10 NaHepes (pH 7.4).

Pipette resistances in normal saline at 18°C were 4–6 MOhms. After filling, pipettes were brought in close contact with the cell surface as rapidly as possible. To minimize flow from the tip, no positive pressure was applied to the pipette before cell contact. In general, seals were rapidly established by suction. The total time from joining tip and shank solutions to gigaseal formation was typically ~80 seconds, although in some cases several minutes were required.

Standard patch clamp recording methods of recording and analysis were employed; the analysis bandwidth was 3–5 kHz. Interval durations were measured by a half-amplitude detection algorithm (IPROC; Sachs *et al.*, 1982) and the reduction of kinetic and amplitude data into histograms and lists was carried out with the aid of an event-list processing program (LPROC; Neil *et al.*, 1991). The reduced data were curve fit with the programs NFITS (C. Lingle, Washington Univ., St Louis, MO) or NFIT (Island Products, Galveston, TX); fitted values are mean +/−s.d.. The infinite sum in Eq. 1a was fitted to seven terms.

For the QX-222 experiments, the mean open channel duration was computed for 10-s segments (open intervals <0.1 ms were excluded from the computation). For experiments regarding ACh-induced blockade, the mean open channel amplitude was calculated in segments that were 10 or 20 s in duration. For kinetic analysis of channel activation, bursts were defined as groups of open intervals separated by closures shorter than some critical duration. Open and closed intervals within an apparently homogeneous subset (H-mode; Auerbach and Lingle, 1986) of all bursts were fitted to a kinetic scheme. Only bursts where one channel was active were analyzed. An interval maximum likelihood method (Horn and Lange, 1983; Horn and Vandenberg, 1984) was used to analyze burst kinetics. To correct for the effects of intervals that went undetected because of limited bandwidth, a new transition matrix (**Q***) was made using a modification of the first-order solution of Roux and Sauve (1985) (Richard Horn, unpublished results):

$$\mathbf{Q}^* = \mathbf{M} + \mathbf{T} \exp(\mathbf{A}t),$$

where **M**, **T**, and **A** are matrices defined in Roux and Sauve. The matrix exponential was calculated by solving the eigenvalues and eigenvectors of the matrix. The rates of a given model were iteratively adjusted under the control of an optimizer that allowed parameters to be constrained (subroutine DNCONF from International Mathematics and Statistics Library, Houston, TX). Bursts were considered to be independent, and the log likelihood values for each burst were simply summed.

In experiments with backfilled pipettes, the time of occurrence of the burst was used to estimate the agonist concentration according to Eq. 1. The salient rates of the transition matrix were scaled by the concentration estimate before calculating the log likelihood. The error limits on the rate estimates were computed from the slope of the likelihood function (Chay, 1988).

To obtain the steady-state calibration curve for the dependence of conductance on the concentration of Na^+ (Fig. 7), pipettes were filled with solutions of different Na^+ concentration (other ions were maintained at their concentration in normal saline) plus 200 nM ACh, and mean open channel amplitude was measured as a function of pipette voltage. The data for the calibration (Fig. 7 *left panel insert*) was obtained by fitting current-voltage curves to straight lines over the range 0 to +60 mV pipette potential.

RESULTS

Diffusion in a pipette

If the assumptions are made that a patch pipettes is conical and that the membrane is at the convergence point, we can quantify diffusion down the tip of a pipette according to spherical geometry, i.e., as radial diffusion from an infinite volume at the surface of a sphere to its center. The concentration of ligand at the membrane patch ($C_m[t]$) as a function of time (t) is given by Eq. 9.3.6 of Carslaw and Jaeger (1959):

$$C_m(t) = (C_s - C_t)\left\{1 + 2\left(\sum_{n=1}^{\infty}(-1)^n \exp(-n^2 t/\tau)\right)\right\} \quad (1a)$$

$$\tau = L^2/\pi^2 D, \quad (1b)$$

where C_s and C_t are the initial shank and tip concentrations, D is the ligand diffusion constant, and L is the fill height of the tip solution (i.e., the radius of the sphere). This equation is subject to the accuracy of the approximation that shank-tip interface is radial and will not be correct for large or nonconstant divergence angles. Note that for small divergence angles, only a single geometric parameter, the fill height L, needs to be determined to define the entire concentration vs. time curve. Note also that the higher order terms of the sum rapidly become negligible, so at long times the concentration of diffusing ligand will increase as a single exponential.

The validity of the approximation that pipettes are cones was tested in two ways. First, pipette geometry was measured directly, with the deviation from a cone measured as a nonconstant divergence angle (Fig. 1 *top*). In my pipettes, the divergence angle increases at a rate of ~3 degree/mm for the first 2 mm from the orifice, above which the tip region flares to join with the shank. From geometry alone, the conical approximation would seem to be adequate if the fill height is < ~2 mm.

The second method of testing the conical approximation was to backfill pipettes with 50 μM carboxyfluorescein (CF), and to monitor the intensity of fluorescence near the tip over time (Fig. 1 *bottom*). The linearity of the light signal as a function of the concentration of CF was confirmed by a calibration curve (insert of Fig. 1). The resulting diffusion profile was fitted by Eq. 1 *a*, with the resulting values τ = 410 +/− 7.2 s, and C_s = 49.9 +/− 0.5 μM CF. In this pipette the value of L was directly measured to be 1.53 mm. From this value we can

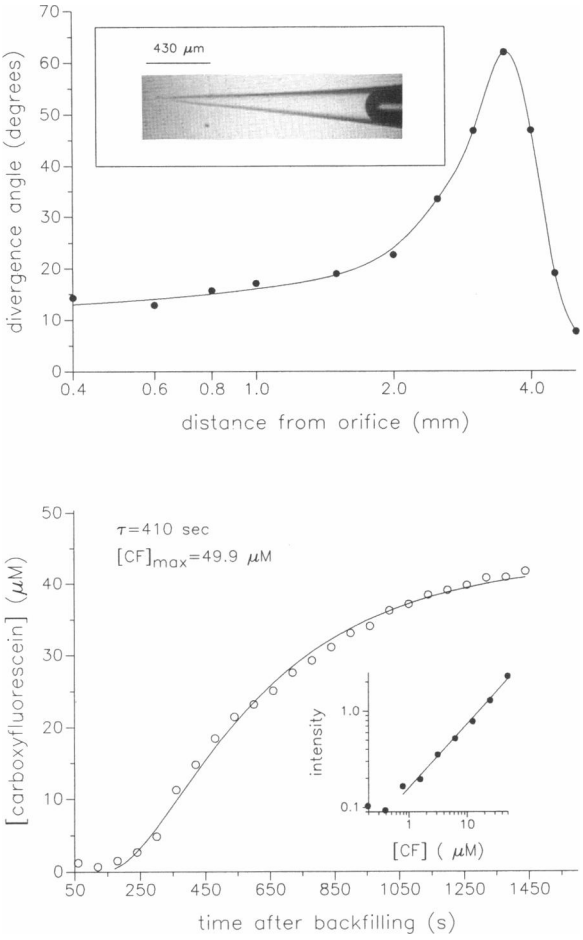

FIGURE 1 Pipette tip geometry. (*Upper*) The divergence angle of the tip region of a pipette plotted as a function of distance from the orifice. The pipette divergence angle increases gradually for ~2 mm and then widens as the tip flares to join the shank. A pure cone would produce a flat line. (*Insert*) image of a typical patch pipette. (*Lower*) Diffusion of carboxyfluorescein (CF) down the tip of a pipette. The tip was filled with CF-free solution and the shank was backfilled with 50 μM CF (24°C). The concentration of CF was estimated from the intensity of the fluorescence and the steady-state calibration curve shown in the insert.

use Eq. 1 *b* to calculate a diffusion constant of 5.78×10^{-6} cm^2 s^{-1} for CF (24°C). The molecular weight of carboxyfluorescein is 376; the estimated diffusion constant is reasonable considering that the diffusion constant (20°C) for sucrose (MW 342) is 4.6×10^{-6} cm^2 s^{-1}. The overall shape of the intensity vs. time curve, the magnitude of the fitted time constant, and the extrapolated limiting concentration of ligand at steady state are in agreement with predictions assuming conical tip region geometry. These results indicate that it is valid to use Eq. 1 to describe diffusion in a patch pipette.

Error analysis

The simple dependence of the diffusion profile on L suggests that if the diffusion constant for the ligand is known, direct measurements of the fill height can be used to obtain the diffusional time constant necessary to transform time into concentration (Eq. 1). Three sources of error with this method of quantitation of the tip concentration over time will be considered: nonconical tip regions, the limited accuracy of the fill height measure, and the formation of seals at significant distance from the conical convergence point.

At some settings of the pipette puller tip regions had cylindrical segments, i.e., regions where the divergence angle drops to zero. The time course of diffusion in a cylinder is substantially slower than that in a cone of equivalent length, thus the presence of cylindrical segments will cause the concentration profile to differ from that described by Eq. 1. To get an estimate of the magnitude of the errors introduced from interposed cylindrical segments I will consider the extreme cases, i.e., tip regions that are either purely cylindrical or conical (Fig. 2 *A*). The error (the difference between the concentrations computed assuming either conical or cylindrical geometry) varies with time and is substantial at early times. For example, if a cylindrical pipette is assumed to conical, the computed concentration will be double the true value at 0.2 τ, about the time recording starts in ACh-filled pipette experiments. While the insertion of a cylindrical segment will certainly produce much smaller errors than in the purely cylindrical case, this result emphasizes the need to establish the conical form of the pipette tip region if the concentrations are to be computed from fill height alone.

A second source of error is imprecision in the measurement of the fill height, L. The time constant varies as the square of the fill height, and the concentration profile varies exponentially with the time constant, so small errors in L may result in significant errors in concentration estimates. In addition to straightforward measurement errors, stirring of the interface during backfilling and/or convective flow from the tip before to seal formation may alter the effective values of L and C_s in ways that cannot be readily quantified a priori, and will thus further reduce the accuracy of the tip concentration estimates.

If the measurement error relative to L is small, the relative error in the computed diffusional time constant will be twice that of the fill height. The magnitude of the error is the difference in computed concentrations for two different diffusional time constants (Fig. 2 *B*). In my experiments, fill heights were measured on a grid superimposed on a video monitor with a resolution of 25 μm.

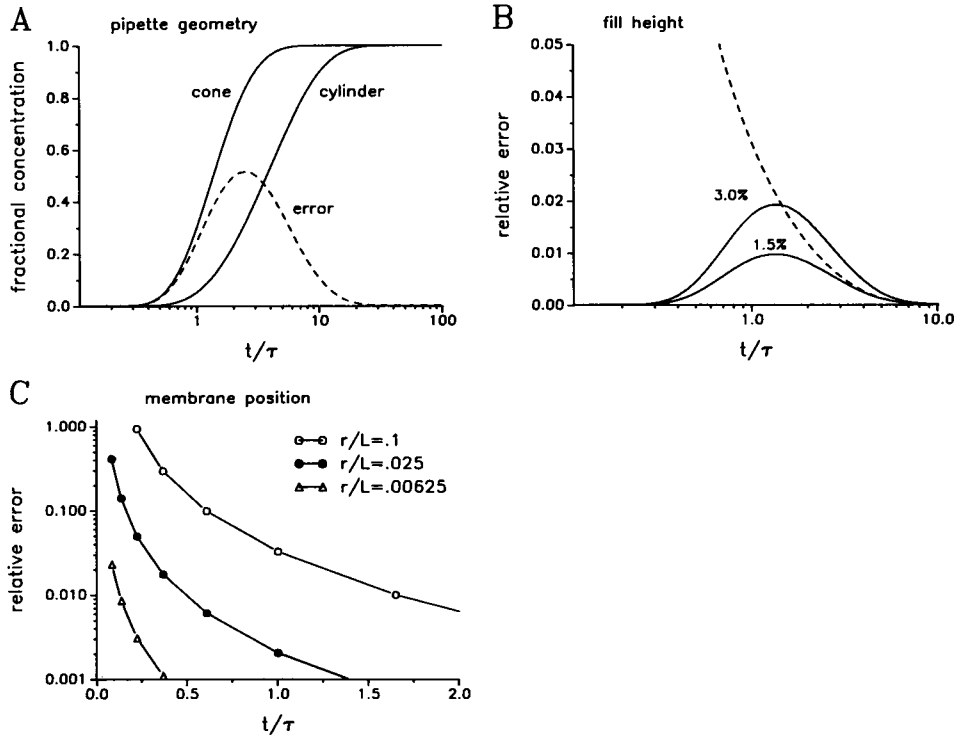

FIGURE 2 Error analysis. (*A*) *Errors in geometry.* The solid lines are diffusional profiles in a pure cylinder or cone with the same fill height; dashed line is the difference in computed tip concentrations, i.e., the concentration overestimate that would pertain if a cylinder was assumed to be a cone. (*B*) *Errors in the fill height measure.* The solid lines are the overestimates in the tip concentration that would pertain given the indicated errors in the computed diffusional time constants. The dashed line is the relative error (as a fraction of the true tip concentration) given a 1.5% error in τ. (*C*) *Errors from the membrane position.* The relative error in the concentration estimate as a function of time for different membrane positions (r = distance from convergence point; L = fill height). For a typical fill height (L = 1.6 mm), the solid symbols would pertain to a membrane 40 μm removed from the convergence point.

To gain an estimate of the magnitude of the error in the concentration estimates arising from errors in L, I will assume an accuracy of 12.5 μm, or, with L = 1.6 mm, a time constant error of 1.6%. This is a worst case estimate, as fill heights were measured with a higher (but unknown) accuracy.

The errors in concentration associated with errors in L decrease with increasing fill heights. With a 1.5% error in τ, the relative errors in concentration (expressed as a fraction of the true concentrations at the tip) can be substantial at early times and only become <20% after 0.18τ. With low molecular weight ligands this dead time is about the same as the time required to position the pipette and form a seal.

The final error to be considered arises because the membrane patch is not at the convergence point of the cone. With a divergence angle of 15 degrees and an orifice radius of 0.5 μm, the true convergence point is ~3.8 μm beyond the orifice. More importantly, light and electron microscopic examination of patches has shown that the relevant membrane may be many tens of microns removed from the orifice (Ruknudin et al., 1991). Therefore the estimates of the concentration gained by the use of Eq. 1 will always be greater than the true values.

The magnitude of the error arising from the approximation that the membrane is at the convergence point of the cone can be calculated by using Eq. 9.3.4 of Carslaw and Jaeger (1959), which gives the concentration as a function of both time and distance from the convergence point (r):

$$C_m(t) = (C_s - C_i) \cdot \left(1 + (2/\pi x)\left\{\sum_{n=1}^{\infty} [(-1)^n/n] \sin(n\pi x) \exp(-n^2 t/\tau)\right\}\right)$$

$$x = r/L.$$

The calculated magnitudes of the overestimates of the tip concentration are shown in Fig. 2 *C* for different relative membrane positions, expressed as different r/L

ratios. The overestimates in the concentration decrease steeply with time after backfilling. Assuming a (perhaps) worst-case distance of 40 μm from the membrane to the true convergence point, and given a typical fill height of 1.6 mm, the calculated errors are <10% of the correct values at times greater than ~0.16τ (with ACh, ~70 s) after backfilling.

To summarize, errors in the shape of the pipette, the measurement in the fill height, and the location of the membrane patch will contribute to errors in the estimated tip concentrations. The magnitudes of these errors are larger at early times and with small fill heights, and, using the procedures outlined in the Methods section, should be <10% during the period of recording single-channel currents. As a rule of thumb, a dead time of 0.2 time constants should be imposed to insure reasonable accuracy in the concentration estimates.

The experimental data presented below suggest that the net inaccuracy in the computed concentrations at the membrane is sufficiently small to allow dose-response curves to be compiled over a range of concentrations that can span several orders of magnitude.

Channel block by QX-222

The first example of the use of a backfilled pipette method is shown in Fig. 3, where the pipette tip was filled with 0.2 μM ACh in normal saline and the pipette shank was backfilled with a solution of 0.2 μM ACh plus 50 μM QX-222, a well known blocker of muscle cell cholinergic channels (Neher and Steinbach, 1978). The kinetic scheme for channel block dictates that the open channel lifetime (t_0) should decrease in direct proportion to the concentration of QX-222 [$C_m(t)$]:

$$C_1 \underset{\alpha'}{\rightleftharpoons} O_2 \overset{k_{block}}{\rightleftharpoons} C_3$$

$$t_0 = (\alpha' + C_m(t) \cdot k_{block})^{-1}. \quad (2)$$

The decrease in the open channel lifetime with time caused by the diffusion of QX-222 to the membrane can be seen in Fig. 3 *A*. The data collection started 90 s after backfilling (dislodging the bubble that separated the shank and tip solutions). Over the next 10 min, the open channel lifetime decreased from ~4 to ~1 s.

The data in Fig. 3 *A* were fitted by a combination of Eqs. 1a and 2, with three unknown parameters to be determined (τ, α′, and k_{block}).

In this example, τ can be estimated from the open duration profile itself, i.e., without prior knowledge of the fill height. The fitted value for the diffusional time constant was 479 +/− 34 s. The fitted values for the rates, obtained from the initial and final limiting values of the t_0 vs. time data, were $\alpha' = 256 +/- 9.6\ s^{-1}$ and

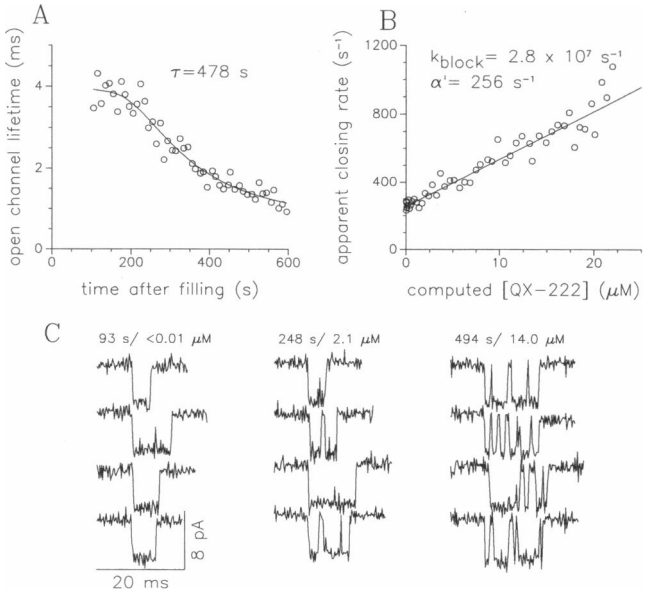

FIGURE 3 Channel block by QX-222. The pipette tip was filled with ACh only and the shank was filled with ACh plus 50 μM QX-222. (*A*) *Time-response profile.* Open channel lifetime decreases as QX-222 diffuses to the tip with a time constant of 478 s. (*B*) *Dose-response profile.* The data in *A* transformed into a dose-response curve according to Eqs. 1 and 2. The membrane potential was −140 mV. (*C*) *Sample single-channel records.*

$k_{block} = 2.8 +/- 0.5 \times 10^7\ M^{-1}s^{-1}$. It is noteworthy that τ can be estimated from just the initial portion of the t_0 vs. time curve; a fit to data where $t < 300$ s yields an estimate of τ of 457 +/− 118 s, similar to (but less precise than) the fit to the entire data set.

Fig. 3 *B* shows the time-dependent data of Fig. 3 *A* recast as a dose-response curve. Eq. 1 was used to convert time into concentration; the effective closing rate is just the inverse of the apparent open channel lifetime. The linear dependence of the apparent closing rate on the concentration of QX-222 is clear and supports the conclusion that the errors in the concentration estimates are minimal.

In a different experiment a pipette filled to a height of 1.6 mm produced an apparent τ of 542 s, or, according to Eq. 1 *b*, a diffusion constant for QX-222 at 18°C of $4.8 \times 10^{-6}\ cm^2\ s^{-1}$. If τ can be estimated from the data itself, the backfilled pipette method can be used to estimate the diffusion constant (molecular size) of the salient ligand.

Activation of AChR

In the series of experiments, pipettes were filled at the tip with normal saline and then backfilled with 5 mM ACh. As ACh diffuses to the tip, the mean current will

first rise as the ACh binds to and activates receptors, but will then decrease as receptors desensitize. In addition, at very high concentrations of ACh the single channel current amplitude will decrease because of unresolvably fast channel block by ACh.

Fig. 4 shows the mean current for two experiments, with fill heights of 1.3 and 2.0 mm. As expected, the current vs. time data (Fig. 4 *A*) shows that the peak current was reached sooner after backfilling in the pipette with the shorter fill height (75 s vs. 176 s). The dose response transform of these data is shown in Fig. 4 *B*, where the mean current has been divided by the single channel amplitude and the time constant has been estimated from Eq. 1 *b* assuming an ACh diffusion constant of 0.6×10^{-5} cm^2 s^{-1} (Dionne, 1976). Despite the very different temporal profiles in these two experiments, the dose-response data are quite similar in form, with the peak activity generated at ACh concentrations of 2.75 and 2.85 μM in the small and large fill height pipettes. (The difference in peak amplitude between the two patches reflects the different number of activatable channels that were present; if we use the rate constant estimates derived from the patch shown in Fig. 6, there were 53 and 41 channels active at the peaks.) Overall, in five experiments under identical experimental conditions except for fill height variations (range: 1.3–2.0 mm; mean: 1.6 mm), the shapes of the dose-response curves were highly congruent. These data are not suitable for quantitative analysis because desensitization is not in steady state relative to the diffusional time constant. However, the close agreement between patches of different fill heights indicates that the simple use of this parameter to calibrate diffusional profiles is adequate, and that errors associated with turbulence at the tip-shank interface and from convective flow from the pipette before seal formation are small.

The effect of increasing ACh concentration on the amplitude of the single channel current is shown for the same two patches in Fig. 5. Again, the rate of decrease in amplitude is greater for the short fill height pipette, but the transform into a dose-response curve brings the time-varying data into alignment. These dose-response data can be fitted by assuming a simple two state kinetic model for blockade:

$$i/i_o = [1 + C_m(t)/K]^{-1}, \quad (3)$$

where i is the normalized amplitude, i_o is the normalized amplitude in the absence of blocker, K is the equilibrium dissociation constant for block, and $C_m(t)$ is the concentration of blocker. Again using 0.6×10^{-5} cm^2 s^{-1} for D_{ACh}, the fitted values for K are 4.5 and 4.9 mM for the pipettes with fill heights of 1.3 and 2.0 mm. These values are in reasonable agreement with those reported for other muscle cell ACh-activated channels (e.g., 6.5 mM at 11°C, −50 mV in BC_3H_1 cells; Liu and Dilger, 1991).

At concentrations of ACh > ~2 μM, currents from muscle cell cholinergic receptors occur in bursts as channels enter and leave desensitized states (Sakmann *et al.*, 1980). In *Xenopus* myocytes, the distribution of closed intervals within bursts in this range of ACh concentrations is dominated by a single exponential

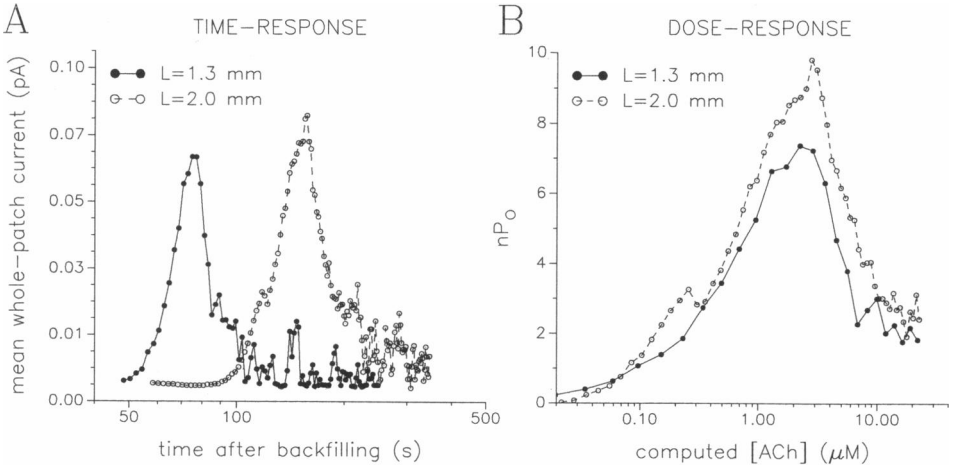

FIGURE 4 Whole-patch dose-response curves for ACh-activated channels. Two experiments are shown where the pipette was backfilled with 100 μM ACh. (*A*) *Mean whole-patch current as a function of time (note log axis).* As expected from Eq. 1b, the peak currents occur at times (75 and 176 s) that can be predicted from the square of the fill heights (L = 1.3 and 2.0 mm). (*B*) *Dose-response transform, according to Eq. 1.* Mean currents have been divided by the single-channel current amplitudes (corrected according to Eq. 3). The peaks essentially superimpose on the concentration axis but are of different amplitude because of a greater number of channels in the pipette with L = 2.0 mm.

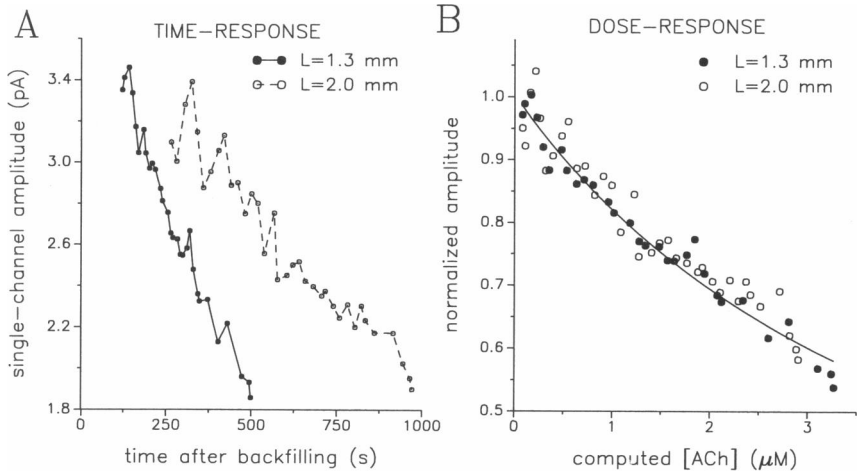

FIGURE 5 Reduction in channel amplitude from ACh blockade. Same experiments as in Fig. 4. The disparate time responses (*A*) come into alignment on the concentration axis (*B*), with K_D for block of 5.0 mM (*B*, solid line).

which has a characteristic rate constant (β') that scales with the concentration of ACh in the range 10–100 μM (Auerbach and Lingle, 1987). This component of the closed interval duration distribution largely reflects the time required by a channel to bind two agonist molecules and open.

In the experiment shown in Fig. 6, the tip was filled to a height of 1.75 mm (τ = 517 s) with normal saline, and the shank was filled with saline plus 100 μM ACh. The rise and fall in the mean current is shown both as a function of time and computed ACh concentration in Fig. 6 *A*. Clear bursting behavior was apparent ~300 s (~5 μM) after backfilling. The decrease in the intraburst closed interval durations as a function of time (increasing concentration) can be seen in the current traces in Fig. 6 *B*. β', obtained by fitting histograms of intraburst closed interval durations, is plotted as a function of the ACh mean ACh concentration over the segment of the record from which intervals were accumulated in Fig. 6 *D*.

Although the concentration of ACh as a function of time can be defined, the problem of how to fit the ever-changing channel kinetics to a kinetic model remains. The minimum acceptable scheme for the activation of a cholinergic channel is:

$$C_1 \underset{k_{21}}{\overset{k_{12}}{\rightleftharpoons}} C_2 \underset{k_{32}}{\overset{k_{23}}{\rightleftharpoons}} C_3 \underset{\alpha}{\overset{\beta}{\rightleftharpoons}} O_4,$$

where C_1, C_2, and C_3 are vacant, monoliganded, and doubly liganded closed states, and O_4 is the lone open state. Open channel block can be ignored (under these experimental conditions) because sojourns in blocked states that are long enough to be detected are rare.

In estimating rate constants for the experiment shown in Fig. 6, I also made the simplifying assumptions that the binding steps are independent and identical (i.e., $k_{12} = 2 \cdot k_{23}$ and $k_{32} = 2 \cdot k_{21}$). Thus, only four rates remain to be determined: k_{23} (single-site agonist association), k_{21} (single-site dissociation), β (channel opening), and α (channel closing).

For interval likelihood analysis, the likelihood of obtaining the observed sequences of open and closed intervals within bursts is maximized by adjusting the rate constants of the kinetic model (Horn and Lange, 1983). Since each burst must start with an opening, the starting point in these calculations is always at state O_4. To account for the ever-increasing concentration of ACh during the course of the recording, the rates k_{12} and k_{23} were multiplied by the concentration of ACh, which was estimated from the burst starting time. Because the burst duration (~150 ms) is short compared with τ(~500 s), it is valid to assume that the concentration of ACh is approximately constant within a burst. Thus, the rate matrix is used for the likelihood computation is updated for each burst, and the likelihood of observing the entire data set is maximized by adjusting the values of k_{23}, k_{21}, β, and α.

The likelihood profile for each of rates are shown in Fig. 6 *C*. The fitted values in this experiment were k_{23} = 121 +/− 1.1 × 10^6 s^{-1} M^{-1}, k_{21} = 2,973 +/− 74.3 s^{-1}, α = 706 +/− 10.3 s^{-1}, and β = 14,179 +/− 291 s^{-1}. The estimated single-site K_D for ACh at 18°C, −115 mV, is 24.6 μM.

The ACh diffusion experiment can be recast as a dose-response curve, where τ is used to convert time into concentration, and where the rate estimates can be used to compute the eigenvalue that corresponds to β'. The

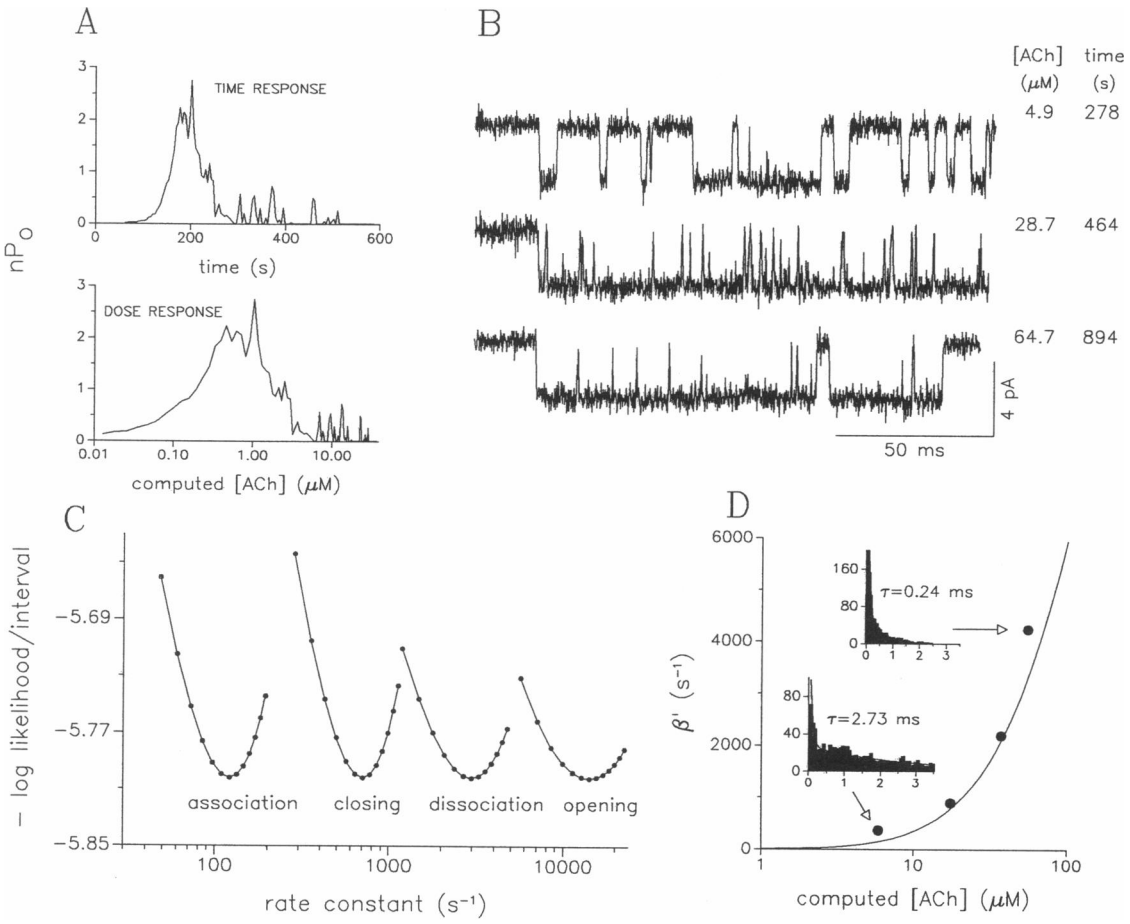

FIGURE 6 Kinetic analysis of cholinergic receptors from a single patch. The pipette was filled to 1.6 mm with saline only and was backfilled with 100 μM ACh. (*A*) Time- and dose-response profiles. (*B*) Sample single-channel data, from bursts that occurred at the indicated concentrations/times. Intraburst gap durations decrease at higher ACh concentrations. (*C*) The likelihood profiles for the estimated rate constants (note log axis). (*D*) The effective opening rate *vs.* the computed concentration of ACh. The symbols were obtained from fitting histograms of intraburst closed intervals (*inserts*); the solid line is not a fit but has been computed from the optimized rate constants (*C*).

resulting single-patch dose response curve for the activation of cholinergic channels by ACh is shown in Fig. 6 *D*. Note that the solid line is not a fit to the histogram data but rather has been computed from the likelihood optimization results. In this patch the probability of being open was equal 0.5 at an ACh concentration of ~7.5 μM, similar the value reported for these channels at 24°C (Auerbach and Lingle, 1987).

Modulation of conductance by Na^+

Current is approximately linear with the concentration of permeant ions only over a limited concentration range. More generally, nonlinear relationships should be taken into account, i.e., saturation in the conductance and changes in the driving force. The next example is an attempt to deduce dose-response parameters for channel conductance from a backfilled pipette experiment.

As Na^+ diffuses to the tip, three processes will significantly influence the channel current amplitude: the channel conductance will increase to some saturating value (Horn and Patlak, 1980), the zero current potential for the channel will increase from a negative to a positive value, and an initial junctional diffusion potential that arose from the ion concentration difference between shank and tip solutions will disappear. These effects can be quantified according to the following equations, which assume a perfectly nonselective cation channel:

$$i = (V_m + V_r + V_j) \cdot (\gamma_m/(1 + K_m/[Na]))$$
$$V_r = 25 \cdot \ln([Na]/120)$$
$$V_j = A \cdot 25 \cdot \ln(N_s/[Na]), \quad (4)$$

where i is the channel current at time t, V_m is the membrane potential (assumed to be constant), V_r is the

reveral potential, V_j is the junctional diffusion potential, γ_m is the maximum conductance, K_m is the concentration of Na^+ producing a half-maximal conductance, [Na] is the Na concentration at time t, N_s is the shank concentration of Na, and A is a term that reflects the different mobilities of Na^+ and Cl^- and is approximately equal to -0.2 (Cole 1972; Moore 1972). With the species and concentrations of ion used here, V_j is significant only at low concentrations of Na, decreasing from 12 mV at 40 mM to 4 mV above 100 mM. The overall effects of the inclusion of changes in V_r and V_j with the concentration of Na^+ is to linearize the conductance vs. concentration curve, i.e., to increase current amplitudes at both high and low concentrations.

The analytical procedure is to transform time into concentration with Eq. 1, then to fit the transformed data to Eq. 4 to obtain estimates for γ_m and K_m. In the experiment shown in Fig. 7 the pipette tip was filled to a height of 1.65 mm with 40 mM Na and was backfilled with 450 mM Na^+ (50 nM ACh in both solutions); the fill height corresponds to a τ of 186 s. The current amplitude is shown as a function of time in the left panel of Fig. 7. These data directly fitted by Eq. 1a produce an erroneous diffusion time constant estimate of 125 +/− 5.3 s. This value is less than that calculated from the fill height because the current vs. Na^+ profile is sublinear.

The right panel of Fig. 7 shows the amplitude data transformed according to Eq. 1 (τ = 186 s). When fitted by Eq. 4, these data yield estimates of 63.5 +/− 1.3 pS for γ_m, and 108.0 +/− 7.7 mM for K_m. These values can be compared with parameters obtained in experiments where pipettes were filled throughout with solutions of different Na concentration (*left panel, insert*). In these steady-state experiments, with fitted values for were 64.8 +/− 16.3 pS and 117.2 +/− 76.2 mM, in good agreement with those obtained in the backfilled pipette experiment.

It is important to emphasize that errors in the fill height measure produce errors in the estimated concentrations that produce still more errors in fitted parameters. For example, in the data of Fig. 7, increasing the height estimate to 1.7 mm produces a drop in K_m and γ_m to 89.6 mM and 62.4 pS, and decreasing the height value to 1.6 mm produces an increase in these values to 138.1 mM and 66.2 pS. For this particular function (Eq. 3), an error of 50 μm (3%) in the fill height measure causes ~30% error in the K_m estimate. Thus the error limits obtained from the fit to Eq. 4 are underestimates.

DISCUSSION

In any dose-response experiment it is important to minimize scatter in both the dose and response measures. In single-channel studies, the response measure, e.g., kinetic or amplitude properties of channel currents, can have scatter that arises from channel heterogeneity. One way to reduce this "extra" variance is to study as few channels as possible by limiting the experiment to a single cell, a single patch, or perhaps even a single channel. Scatter in the dose parameter is ordinarily not an issue, as the concentration of the ligand is typically under tight experimental control. Undoubtedly, if channel activity is robust and if patch excision does not significantly alter channel behavior, then superfusion of outside- or inside-out patches affords the least scatter in

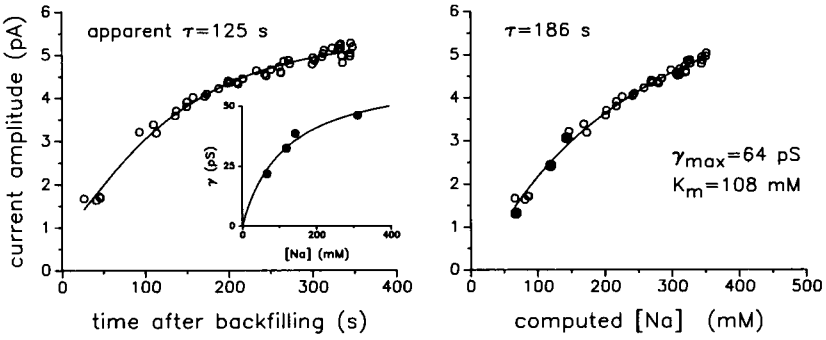

FIGURE 7 Diffusion of Na influences channel amplitude. The tip was filled with 40 mM NaCl saline and the shank was filled with 450 mM NaCl saline (other ions equal; 50 nM ACh throughout). (*Left*) Channel amplitude increases as Na^+ diffuses to the tip. Without considering saturation in the channel conductance and changes in the driving force, the data fitted by Eq. 1 gave an erroneous time constant of 125 s. (*Insert*) Steady-state calibration curve showing the saturation in channel conductance with increasing [Na]. The solid line is the fit to the data with K_m = 65 pS and γ_m = 117 mM. (*Right*) The dose response transform of the data in the left panel after considering conductance and driving force according to Eq. 3. The fitted K_m and γ_m values are similar to those obtained from the steady-state experiments shown in the insert of the left panel. Open symbols are from the backfilled pipette experiment; solid symbols are computed from the steady-state calibration experiments.

both concentration and current parameters and is the preferred method for carrying out dose-response studies on single patches.

In the diffusional delivery dose-response method, ligand diffuses from the shank to the tip of a patch pipette. The main advantage of this method is that the dose-response studies are carried out on single patches in the cell-attached mode where cell metabolism is maintained and the disruption of the membrane is minimal. A side benefit is that no perfusion apparatus is needed.

An added advantage of the diffusional delivery method is that one is forced to analyze all of the data at once, i.e., to fit the entire dose-response curve to a single quantative model. In the examples described above, block by QX-222 (Fig. 3) or ACh (Fig. 5), activation of receptors by ACh (Fig. 6), and modulation of current amplitude by Na^+ (Fig. 7), the salient parameters were estimated from the entire response profile obtained from at least an order of magnitude range of ligand concentration. This treatment of the data as a whole rather than in parts greatly constrains the optimization process and results in a faster convergence to, and more accurate estimates of, the fitted parameters. Of course, similar analyses of entire dose-response curves is possible in steady-state patch experiments.

The maximum likelihood method of kinetic analysis is a natural complement to the diffusional delivery method. All of the kinetic data is used as effectively as it would be in stationary experiments, and the computational overhead associated with rescaling and solving the rate matrix for each burst is not great. This pseudo-stationary approach could be extended to include interval-by-interval updates, but for cholinergic channels this is unnecessary because diffusional time constants are more than 1,000 times longer than burst durations thus the concentration during a burst can be assumed to be constant. An alternative to the interval likelihood method may be to make histograms of interval durations for segments of the record (e.g., 30 s epochs), but, for kinetic analysis, the data density would likely be too low for binning to provide a significant computational advantage.

The main drawback to the diffusional delivery method is that errors are introduced in the measurement of the dose and thus in the estimated parameters. Although these errors are minimal after ~ 0.2 diffusional time constants, it may be possible to use some aspect of the channel currents themselves to calibrate each pipette to further reduce the errors in the estimates of ligand concentration. For example, varying the concentration of a permeant ion (over a limited range that does not effect kinetic parameters) can result in readily quantifiable changes in current amplitude that might serve as an internal calibration. If pipettes were backfilled with both an ion and a drug, the drug concentration could be deduced from the current amplitude because the τ value of the drug and that of the ion are inversely related by their diffusion constants. However, with diffusional delivery there will always be more uncertainty in the dose than in steady-state experiments.

A second limitation of the method is that both the diffusion rate and concentration range are limited because they are determined by a single experimental parameter, the fill height. Some flexibility is afforded by altering the length of the tip region and/or the time the tip is placed in the filling solution. With Na^+ as the diffusing ligand (18°C), I have obtained τ values ranging from 60 to 300 s, with a mean ~ 180 s. Errors at early times and the time required to make a seal set the lower limit on τ, while the persistence of channel activity and the stability of cell-attached patches set its upper limit. It is important to emphasize that the use of Eq. 1 to describe the diffusional profile requires that the tip-shank interface be in a concial region, i.e., pipettes with tips filled into the shank region will not produce the form characteristic of radial diffusion.

The method of diffusional delivery might be extended to whole-cell experiments. The time dependence of the concentration of ligand at the pipette orifice could be combined with estimates of diffusion through the orifice, within a cell, and across the membrane (Pusch and Neher, 1988; Mathias et al., 1990) to yield a profile of intracellular ligand concentration. In this way dose-response studies of channels that are modulated by intracellular ligands could be carried out on single cells.

In summary, the backfilled patch pipette technique is a convenient method for generating dose-response curve in single patches. To minimize errors in the tip concentration estimates, fill height should be measured with an error of <25 μm, and data acquired earlier than ~ 0.2 diffusional time constants should be discounted. With a typical fill height of 1.6 mm, small molecules (e.g., ACh) will have time constants around 7 min, while larger proteins (e.g., BSA) may have time constants that are over an hour. The technique may prove useful in the quantitation of drug action, and as a probe of drug molecular size.

I thank Dick Horn for kindly providing source code to compute the likelihood function, Sun Xun for computer programming, and Fred Sachs for pointed discussions.

Supported by NS23513.

Received for publication 8 January 1991 and in final form 20 May 1991.

REFERENCES

Auerbach, A. 1991*a*. A method for analysing the concentration dependence of ion channel kinetics in cell-attached patches. *Biophys. Soc. Abstr.*

Auerbach, A., and C. J. Lingle. 1986. Heterogeneous kinetic properties of acetyl-choline receptor channels in *Xenopus* myocytes. *J. Physiol. (Lond)*. 378:119–140.

Auerbach, A., and C. J. Lingle. Activation of the primary kinetic modes of large- and small-conductance cholinergic ion channels in *Xenopus* myocytes. *J. Physiol. (Lond.)*. 393:437–466.

Carslaw, H. S., and J. C. Jaeger. 1959. Conduction of Heat in Solids. Oxford Univ. Press, New York. Second edition. 233.

Chay, T. R. 1988. Kinetic modeling for the channel gating process from single channel patch clamp data. *J. Theor. Biol.* 132:449–468.

Cole, K. S. 1972. Membranes, Ions and Impulses. Univ. of California Press, Berkeley, CA. 174.

Covarrubias, M., and J. H. Steinbach. 1990. Excision of membrane patches reduces the mean open time of nicotinic acetylcholine receptors. *Pflug. Arch. Eur. J. Physiol.* 416:385–392.

Cull-Candy, S. G., R. Miledi, and I. Parker. 1980. Single glutamate-activated channels recorded from locust muscle fibers with perfused patch-clamp electrodes. *J. Physiol. (Lond.)* 321:195–210.

Dionne, V. E. 1976. Characterization of drug iontophoresis with a fast microassay technique. *Biophys. J.* 16:705–717.

Horn, R., and K. Lange. 1983. Estimating kinetic constants from single channel data. *Biophys. J.* 43:207.

Horn, R., and A. Marty. 1988. Muscarinic activation of ionic currents measured by a new whole-cell recording method. *J. Gen. Physiol.* 92:145–159.

Horn, R., and J. Patlak. 1980. Single channel currents from excised patches of muscle membrane. *Proc. Natl. Acad. Sci. USA.* 77:6930–6934.

Horn, R., and C. A. Vandenberg. 1984. Statistical properties of single sodium channels. *J. Gen. Physiol.* 85:505.

Liu, Y., and J. P. Dilger. 1991. Opening rate of acetylcholine receptor channels. *Biophys. J.* 60:424–432.

Mathias, R. T., I. S. Cohen, and C. Oliva. 1990. Limitations of the whole cell patch clamp technique in the control of intracellular concentrations. *Biophys. J.* 58:759–770.

Moore, W. 1972. Physical Chemistry. Prentice Hall, New York. 435.

Neher, E., and R. Eckert. 1988. Fast patch-pipette internal perfusion with minimum solution flow. *In* Calcium and Ion Channel Modulation. Grinell, A. D., D. Armstrong, M. B. Jackson, editors. Plenum Press, New York.

Neher, E. and J. H. Steinbach. 1978. Local anaesthetics transiently block currents through single acetycholine-receptor channels. *J. Physiol. (Lond.)*. 277:153–176.

Neil, J., Z. Xiang, and A. Auerbach. 1991. List-oriented analysis of single-channel data. *Methods Neurosci.* 4:474–490.

Pusch, M., and E. Neher. 1988. Rates of diffusional exchange between small cells and a measuring patch pipette. *Pflug. Arch. Eur. J. Physiol.* 411:204–211.

Ruknudin, A., J. J. Song, and F. Sachs. 1991. The ultrastructure of patch clamped membranes: a study using high voltage electron microscopy. *J. Cell Biol.* 112:125–134.

Roux, B., and R. Sauve. 1985. A general solution to the time interval omission problem applied to single channel analysis. *Biophys. J.* 48:149–158.

Sachs, F., J. Neil, and N. Barkakati. 1982. The automated analysis of data from single ionic channels. *Pflug. Archiv. Eur. J. Physiol.* 395:331–340.

Sakmann, B. J. Patlak, and E. Neher. 1980. Single acetylcholine activated channels show burst kinetics in the presence of desensitizing concentrations of agonist. *Nature (Lond.)*. 286:71–73.

Tang, J. M., J. Wang, F. N. Quandt, and R. S. Eisenberg. 1990. Perfusing pipettes. *Pflug. Arch. Eur. J. Physiol.* 416:347–350.